Simulation of Concurrent Detonation of Multiple High Explosive Charges

Len Schwer[1], Steven Stojko[2], Huon Bornstein[2]

[1]Schwer Engineering & Consulting Services, USA
[2]Defence Science and Technology Group, Australia

1 Introduction

A 1D spherical LS-DYNA Multi-Material Arbitrary Lagrange Eulerian (MM-ALE) model was constructed to simulate the three single charge events reported in MABS 25 manuscript P-029 Stojko, et al. (2018). These three simulations were repeated using 2D axisymmetric meshes.

Multiple charge simulations were made using 2D axisymmetric and 3D models of the double and triple charge experiments.

As stated by Stojko et al.

> "The primary purpose of the experiments was to provide a database of results for the validation of numerical modeling of the effects from multiple high explosive charges."

The model results presented in this manuscript support this statement of the data representing a valuable validation database for both single and multiple charge explosions.

Single C-4 charge masses of 60, 120 and 180 grams were modeled using a JWL equation of state with parameters taken from the LLNL Explosives Handbook. The air was modeled as an ideal gas using a polynomial equation of state.

A nominal mesh size of 1 mm was used in the 1D simulations as this allows for more than 20 elements across the charge radius for all three charges; the rule-of-thumb is a minimum of 10 elements across the radius. A more refined 0.5 mm mesh was also simulated with no significant differences from the 1mm mesh result for the 1D 60 gram spherical calculation. For the 2D axisymmetric mesh, a 2 mm mesh size was demonstrated to be converged.

The initial 1D spherical results comparison was quite disappointing. Using the standard LLNL Explosive Handbook parameters resulted in pressure pulses arriving later than the data and with a smaller magnitude. In an effort to calibrate the C-4 parameters, the initial internal energy was increased until the maximum pressure better agreed with the data; this also improved the Time of Arrival (TOA) comparisons. Calibration of the initial energy was limited to the single 60 gram charge case, but the same calibration factor was used in all subsequent simulations providing some justification for the calibration.

2 Experimental Setup

The experiments were conducted in an enclosed blast chamber at the Defence Science and Technology (DST) Group. Figure 1 shows an overview of the test setup with three charges suspended from the ceiling and the instrumented target plate immediately below. In addition to reflected pressure measurements, high speed video imaging was also obtained.

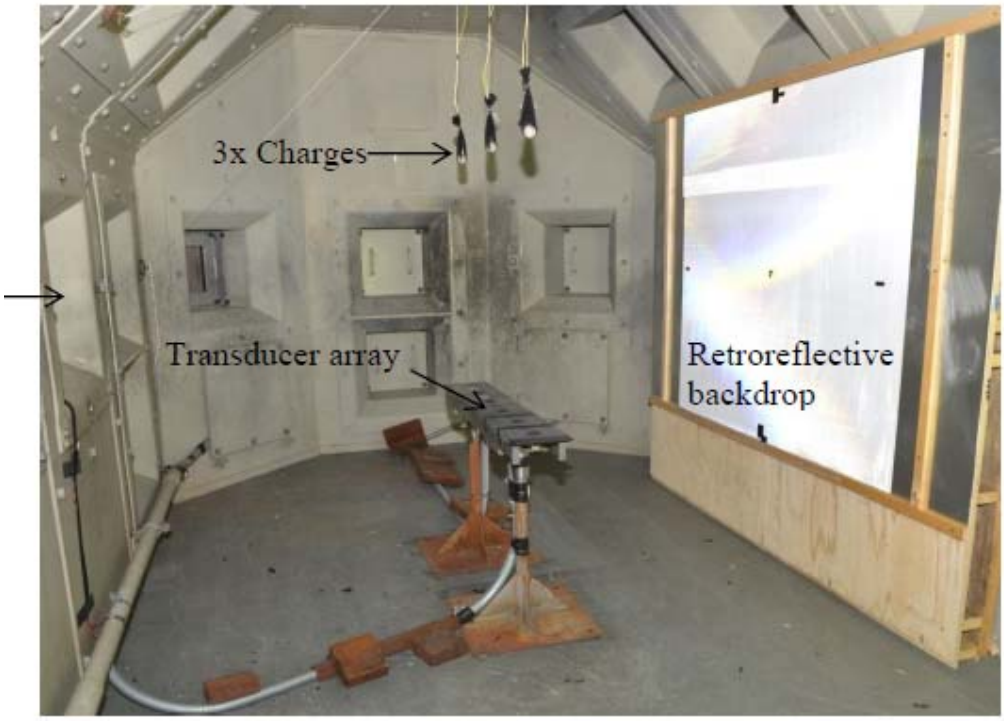

Figure 1 Experimental setup inside the DST blast chamber. (Figure 1 in Stojko et al.)

The reflected pressure transducer array consists of a flat steel plate of dimensions 1.2x0.2 meters with the possibility of 11 active transducers spaced 100 mm apart as shown in Figure 2. The array is located 1 meter below and centered on the middle explosive charge. The paper by Stojko et al. focused on pressure results at the center transducer P6 with video images of the arriving shock waves.

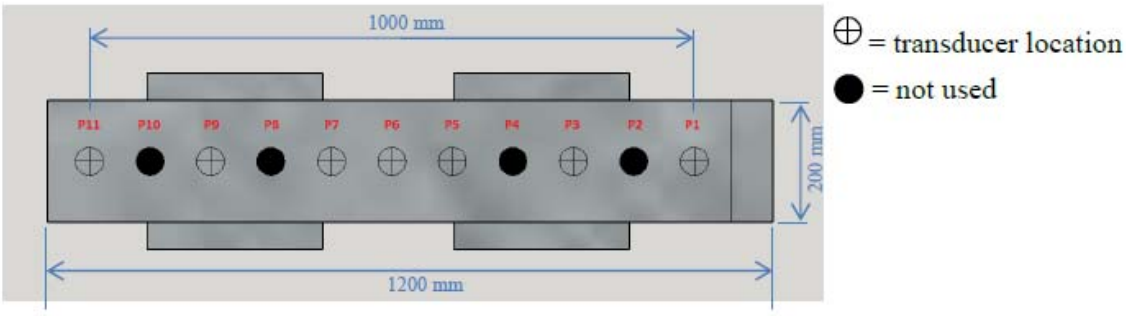

Figure 2 Target array of reflected pressure transducers. (Figure 2 in Stojko et al.)

The spherical charges of Plastic Explosive Number 4 Marked Composition (PE-4 MC), referred to here as PE-4, were bare charges formed in hemispherical molds with a void for the detonator intended for center detonation. The PE-4 charges were cast in three masses:

60 grams with 21.36 mm radius
120 grams with 26.85 mm radius
180 gram with 31.2 mm radius

The test series consisted of six “Events,” see Figure 3, with some replicate tests:

Event 1 – 60 gram charge centered on pressure gauge array at P6
Event 2 – 120 gram charge centered on pressure gauge array at P6

Event 3 – 180 gram charge centered on pressure gauge array at P6
Event 4 – two 60 gram charges separated by 1000 mm, i.e. each centered over the outer pressure gauges at P1 and P11.
Event 5 – three 60 gram charges separated by 500 mm, i.e. centered over the center and outer pressure gauges at P1, P6 and P11.
Event 6 – three 60 gram charges positioned on a 1000 mm radial arc

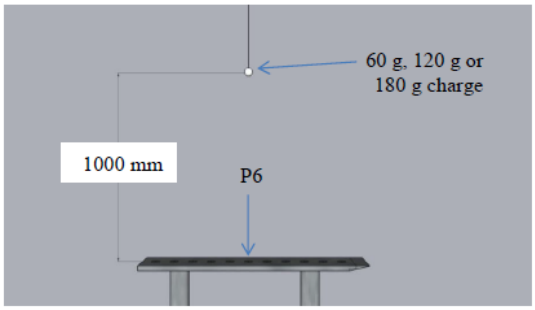

Event 1-3

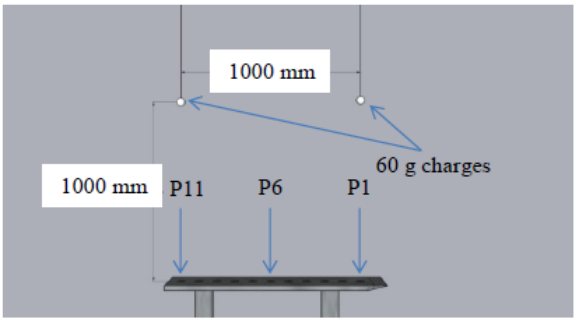

Event 4

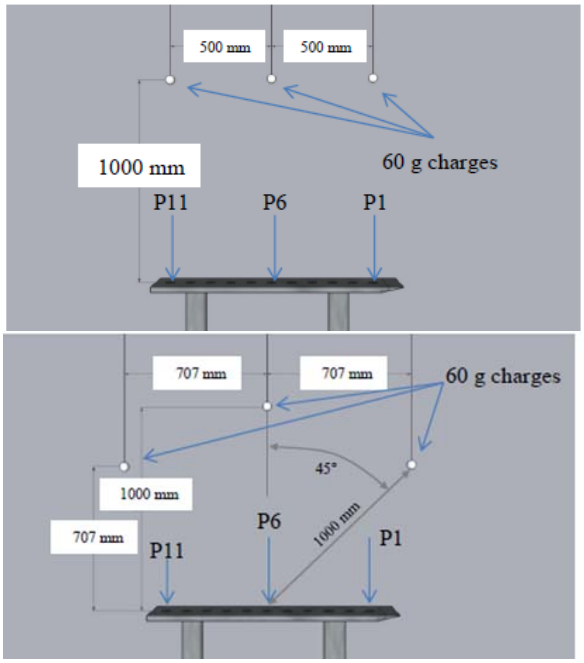

Event 5 Event 6

Figure 3 Schematics of charge configurations for six events. (Figures from Stojko et al.)

3 LS-DYNA Modeling

Multi-Material Arbitrary Lagrange Eulerian (MM-ALE) models were created using a 1D spherical geometry and 2D axisymmetric cylindrical geometry to approximate the explosive charges and reflected pressure transducers. The 1D spherical model consisted of 1000 beam elements of length 1 mm and the 2D axisymmetric model consisted of a computational domain of 1600 mm radius and 1000 mm length of uniform 2 mm quadrilateral elements, see Figure 4. In both models, the location of the reflective pressure target was modeled as nodes constrained from motion normal to the target array. Tracer particles were placed at the corresponding gauge locations to record the reflected pressure histories. Note: spherical (1D) and cylindrical (2D) modeling does not account for clearing effects around the finite dimensioned target, but does allow for capturing the maximum pressure and initial decay which is the primary focus of the measurements.

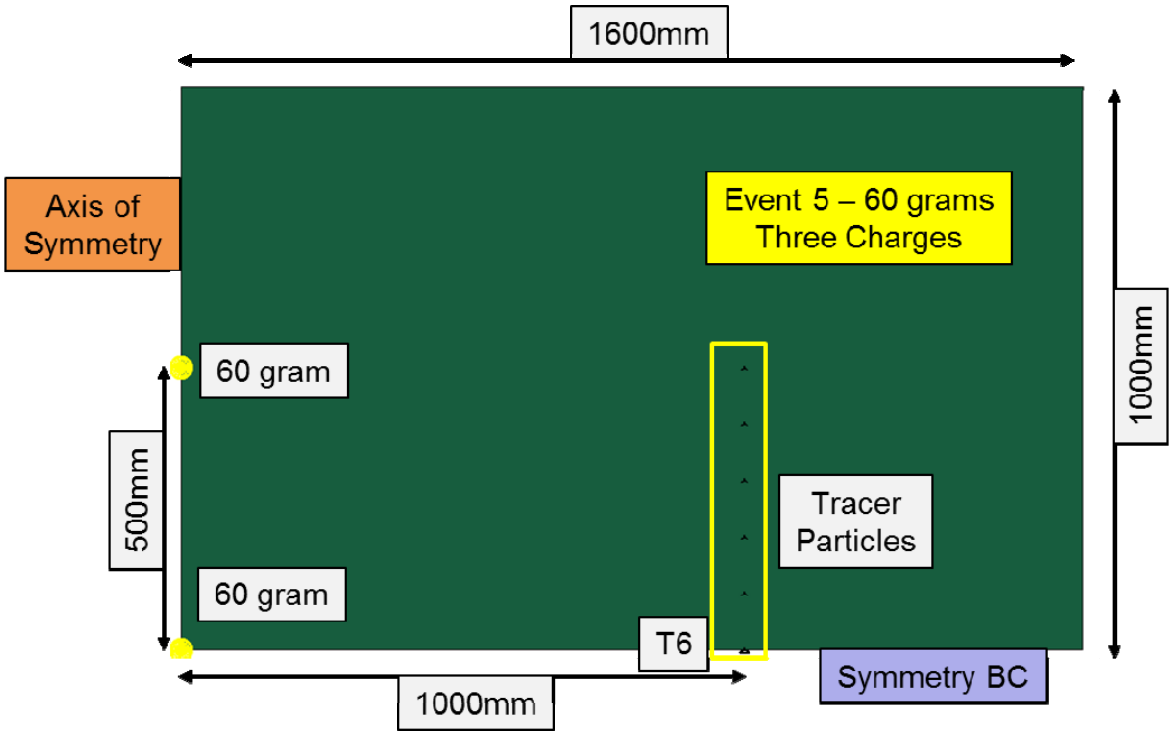

Figure 4 Illustration of 2D axisymmetric model with tracer particle locations.

Mesh refinement studies for the 1D spherical and 2D axisymmetric models are reported in an appendix. It was demonstrated that 0.5 and 1 mm uniform meshes produce essentially identical results for the 1D spherical model, and similarly, 1 and 2 mm uniform 2D axisymmetric meshes produce nearly identical results. Also reported in that appendix are the comparison of 1D and 2D results for Event 1, where it is recommended to use advection method METH=3.

The material and equation-of-state models and parameters for air and C-4 are provided in an appendix.

4 Laboratory Data and Results Comparisons

Before presenting the data and simulation results comparisons, the initial internal energy of the explosive charge is calibrated to the 60 gram charge Event 1 results. The same initial energy calibration is used in all subsequent simulations.

4.1 PE-4 Charge Calibration

Figure 5 shows the comparison of the Event 1 60 gram measured pressure histories, i.e. three repeat tests, there was likely"jetting" from the detonator that caused the odd shape of Repeat 2 test. It is believed this problem was corrected in subsequent testing. Center transducer P6 and the corresponding result from the 1D spherical model; because both 1D spherical and 2D axisymmetric models produced nearly identical results[1], the 1D spherical model will be used in the calibration calculations. As can be seen, the maxima of the measured pressures are larger than that of the simulation, and the measured shocks arrive earlier than the simulation predicted TOA.

[1] See the mesh refinement appendix.

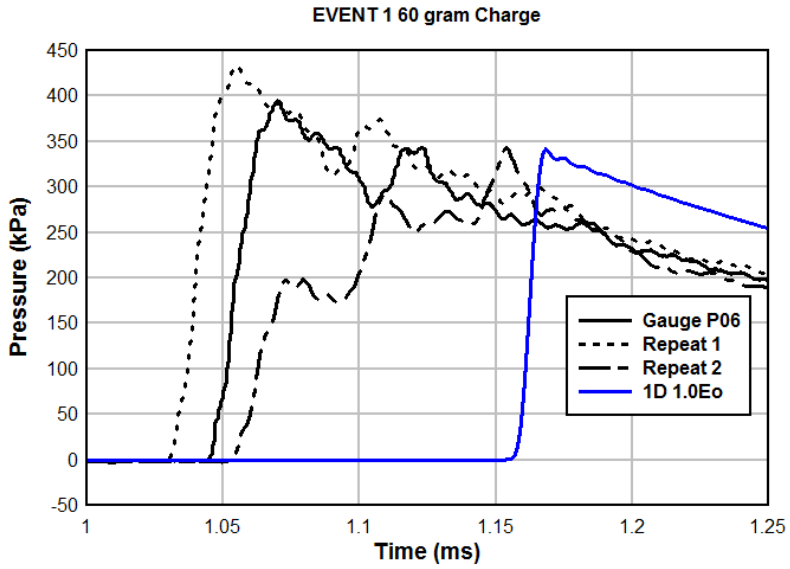

Figure 5 Comparison of measured pressure histories at gauge P6 of Event 1 with the corresponding LS-DYNA 1D spherical result.

While the JWL EOS parameters for C-4 should be close to those for PE-4, see a nice discussion of C-4 and PE-4 equivalence by Bogosian et al. (2016), it is possible that for a particular PE-4 formulation, the handbook C-4 values are not adequate to represent PE-4. In any case, an attempt is made here to calibrate the LLNL Explosive Handbook C-4 JWL initial energy E_0 parameter to the experimental results by increasing the initial internal energy of the explosive. The initial energy is chosen as the calibration parameter as it directly affects both the TOA and maximum pressure, i.e. increasing the internal energy causes a larger maximum pressure and an earlier TOA. The nominal C-4 value for the internal energy is $E_0 = 9$ GPa (5.61MJ for a density of 1601 kg/m^3).

In a parameter study using the 1D spherical model, the internal energy was increased as shown in Figure 6 to an amount 1.4 times the handbook value, i.e. $E_0 = 12.6$ GPa. For this value of the initial energy, the TOA agrees with gauge P06 and the maximum pressure is close to that of Repeat 1. The credibility of this EOS calibration will be tested in subsequent simulations using larger and multiple PE-4 charges.

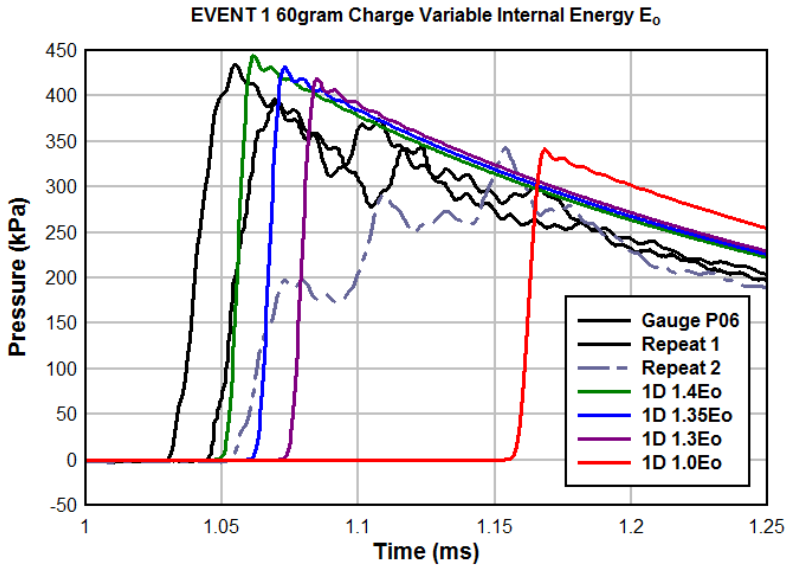

Figure 6 Variation of initial internal energy by increases of 30 to 40%.

Alternative JWL EOS parameters, suggested by Jing Ping Lu of DST, and the ConWep result for 60 grams of C-4 at 1 meter are presented in an appendix.

4.2 Event 1 – Single 60 gram PE-4 Charge

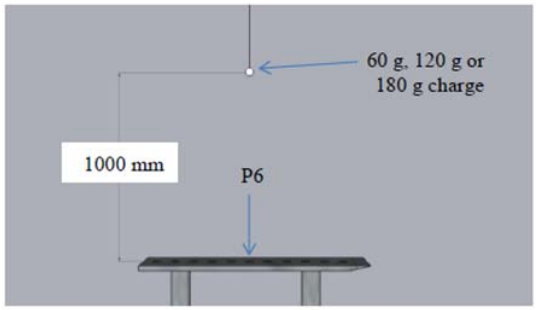

Figure 7 Configuration for Event 1 with centered single 60 gram PE-4 charge. (Figure 8 in Stojko et al.)

Figure 7 shows the initial configuration for Event 1 with a single 60 gram PE-4 charge suspended 1000 mm above the central pressure transducer P6 in the target plate.

The results comparisons for Event 1 are shown in Figure 8. Both the 1D spherical and 2D axisymmetric results are shown as credibility of the 2D axisymmetric model will be needed for simulation of Events 4 & 5. The maximum pressures[2] range from 393, 444 and 409 kPa for P06, 1D and 2D models, respectively, and the TOA range similarly from 1.07, 1.06, 1.09 milliseconds.

As can be seen in Figure 8, the exponential decay of the data and two models are significantly different. As mentioned previously, the data is subject to relief waves from the edges of the finite target plate while the simulation results are not. As for the 1D and 2D simulation decay rates, the 1D

[2] Maximum pressure is the worst metric for comparing pressure histories. Changes in the experimental or simulation sampling rate will affect the reported maximum pressure. Further, for structural analyses, the maximum pressure is seldom used; rather the maximum impulse dominates structural response.

spherical model constraints the lateral air shock in all directions, while the 2D model only constrains the lateral flow in the circular cylindrical direction.

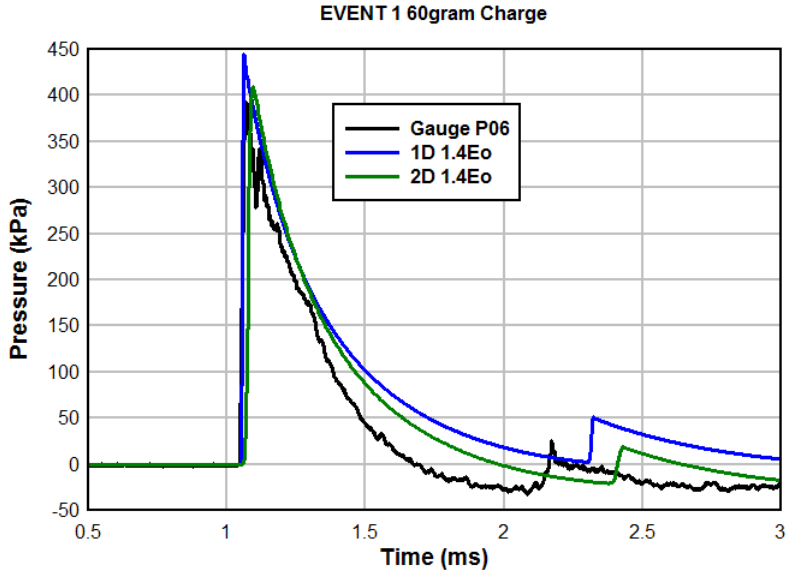

Figure 8 Comparison of pressure histories for Event 1 single 60 gram charge of PE-4.

The negative phase of the data is terminated at about 2.2ms, while for the simulations this time is 2.3ms for the 1D spherical model and 2.4ms for the 2D axisymmetric model. The negative phase is terminated due to the arrival of the recompression or secondary shock. Unlike the incident shock, the secondary shock travels though detonation product and air. The delay in the arrival of the secondary shock in the simulation result is thought to be due to the propagation of that wave through the numerical detonation products, i.e. the gas generated from the JWL EOS, which likely differs from the physical detonation products. Also contributing to the delay of the simulated secondary shock are the confining spherical and cylindrical geometries, e.g. since the spherical geometry has somewhat higher pressures during the decay, the secondary shock will travel faster than through the lower pressure cylindrical geometry.

In addition to the secondary shock, if there are detonation products available to be oxidized with sufficient oxygen and temperature, additional burning can occur, i.e. afterburning. There is no afterburning considered in the simulation results as maximum reflected pressure and initial decay are the focus of the experimental results.

Finally, in an unreported parameter study, it was found that the results agree better with the experiments if the advection method is set to METH=3 “Donor cell with HIS modified to conserve total energy over each advection step, …” as opposed the METH=2 “Van Leer with HIS, second order accurate (default).”

4.3 Event 2 – Single 120 gram PE-4 Charge

The initial configuration for Event 2 with a single 120 gram PE-4 charge suspended 1000 mm above the central pressure transducer P6 in the target plate is the same as shown previously in Figure 7.

The results comparisons for Event 2 are shown in Figure 9. Both the 1D spherical and 2D axisymmetric results are shown. The maximum pressures range from 739, 906 and 811 kPa for P06, 1D and 2D models, respectively, and the TOA range similarly from 0.89, 0.84, 0.88 milliseconds; there was one repeat test for Event 2 with nearly identical maximum pressure of 742 kPa and TOA 0.87ms. For 1D and 2D simulations, the maximum pressure is significantly over predicted by 23 and 10%, respectively. This indicates the calibration of the 60 gram PE-4 charge is not appropriate for the larger 120 gram charge, i.e. a smaller calibration factor is needed. However, since the multiple charge events, i.e. Events 4, 5 & 6, use 60 gram charges, the 60 gram charge mass calibration was selected.

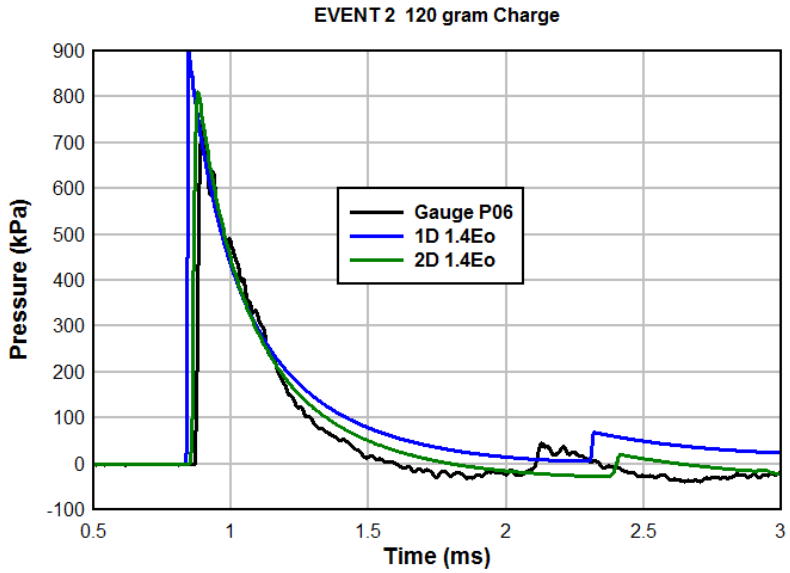

Figure 9 Comparison of pressure histories for Event 2 single 120 gram charge of PE-4.

4.4 Event 3 – Single 180 gram PE-4 Charge

The initial configuration for Event 3 with a single 180 gram PE-4 charge suspended 1000mm above the central pressure transducer P6 in the target plate is the same as shown previously in Figure 7.

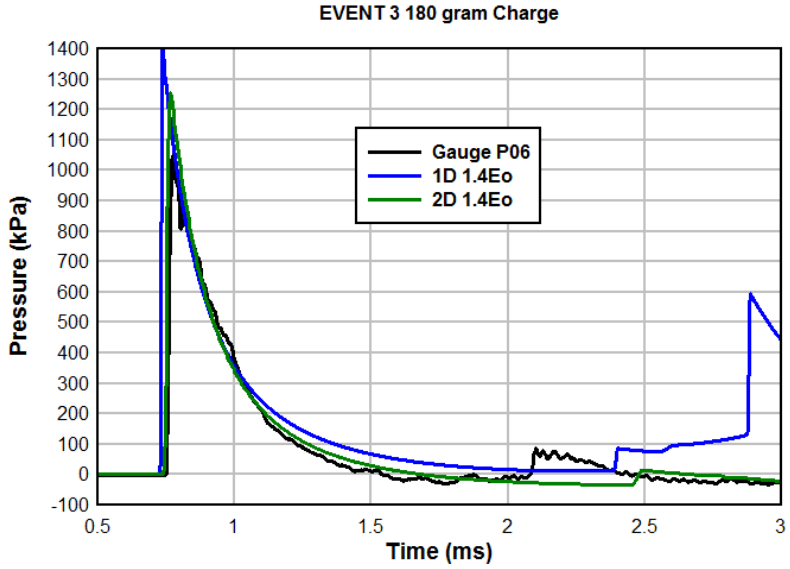

Figure 10 Comparison of pressure histories for Event 3 single 180 gram charge of PE-4.

The results comparisons for Event 3 are shown in Figure 10. Both the 1D spherical and 2D axisymmetric results are shown. The maximum pressures range from 1048, 1410 and 1255 kPa for P06, 1D and 2D models, respectively, and the TOA range similarly from 0.78, 0.74, 0.76 milliseconds; there was one repeat test for Event 3 with somewhat lower maximum pressure of 924 kPa and nearly identical TOA 0.79ms.

For 1D and 2D simulations, the maximum pressure is significantly over predicted by 35 and 20%, respectively. This again indicates the calibration of the 60 gram PE-4 charge is not appropriate for the larger 180 gram charge; as was the case for the 120 gram charge.

The large pressure increase in the 1D spherical result at 3ms is due to the reflection of the secondary shock at 0.74ms traveling back to the center of the spherical charge and propagating back to the constrained 1000 mm location.

4.5 Event 4 – Two 60 gram PE-4 Charges

The initial configuration for Event 4 with two 60 gram PE-4 charges suspended 1000 mm above the outer pressure transducers, P1 and P11, in the target plate is shown in Figure 11.

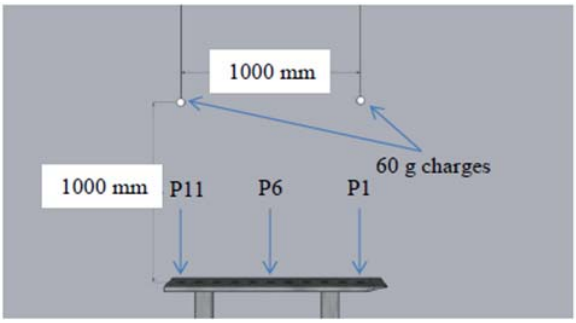

Figure 11 Configuration for Event 4 with two 60 gram PE-4 charges. (Figure 12 in Stojko et al.)

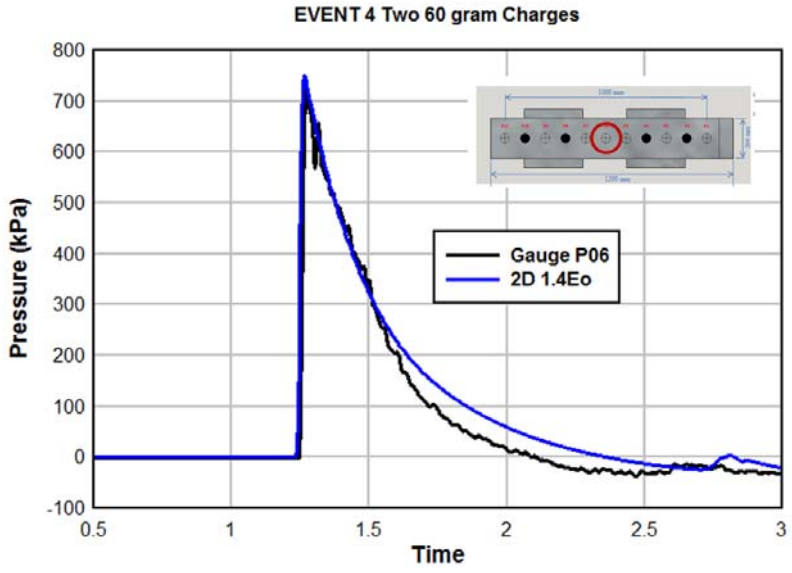

Figure 12 Comparison of pressure histories for Event 4 two 60 gram charge of PE-4 at the center gauge P06.

The result comparisons for Event 4 are shown in Figure 12. Only 2D axisymmetric results are possible for this multi-charge configuration. The maximum pressures are 729 and 750 kPa for P06 and the 2D model, respectively, and the TOA are similar with 1.27 and 1.26 milliseconds.

There was no repeat test for Event 4, but the two end gauges P01 and P11 serve as duplicate measurements due to symmetry. Note: the target plate is not exactly symmetric with respect to the gauges. The free end near the gauge P1 is 130 mm and the end near gauge P1 is 70 mm. This small

difference was ignored in the simulations. Figure 13 shows the two end gauge pressure histories and the 2D axisymmetric simulation result. The average maximum measured pressure is 312 kPa and the simulation maximum pressure is 409 kPa or 31% larger. The TOAs are similar with 1.1ms for the measurements and 1.09 for the simulation.

Note the maximum pressure at the center gauge P06 is almost double that at the outer gauges P01 and P11, since the center gauge is subjected to the combined pressure from the two symmetric charges. The large pressure pulse at the outer gauges that occurs at about 2ms is due to the lateral motion of the combined central pressure shock moving outward along the target plate and this pressure magnitude is well predicted by the simulation.

The question is how the central gauge, P06, can only differ my 3% for maximum pressure while the ends gauges differ by 31% between the measured and computed results. No answer is presently available.

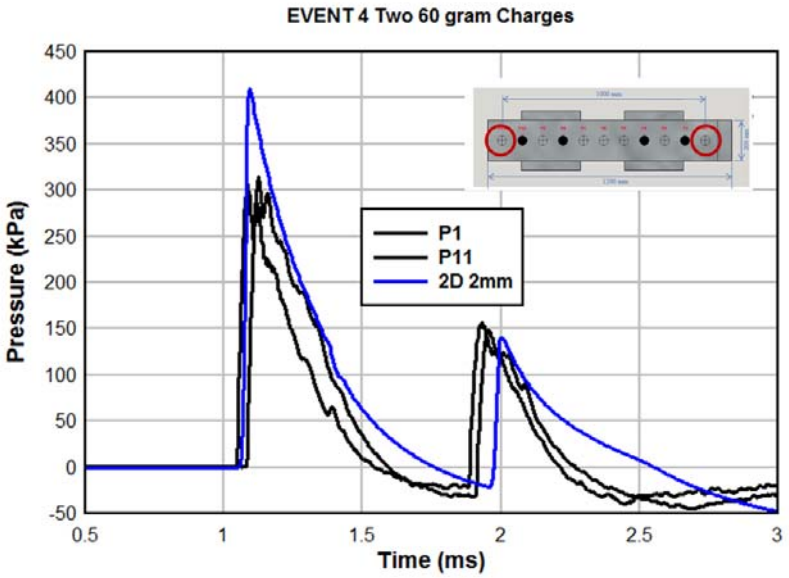

Figure 13 Comparison of pressure histories for Event 4 two 60 gram charge of PE-4 at the end gauges P01 and P11.

As mentioned previously, video of the events was also recorded in the form of high speed shadowgraphs; several frames from the videos are provided in the Stojko et al. paper. These images can be compared with digital Schlieren images created by post processing from fluid density fringes. Stojko et al. provide this comment on such comparisons:

> "However, if these results are to be compared with results from numerical modelling then care must be taken to ensure that the correct plane of reference is used. Numerical results are often viewed in a single plane, whereas the shadowgraph images are a two dimensional view of a three dimensional phenomenon."

With that cogent comment in mind, Figure 14 presents a comparison of the Event 4 shadow graph at 1ms with the corresponding LS-DYNA base Schlieren image.

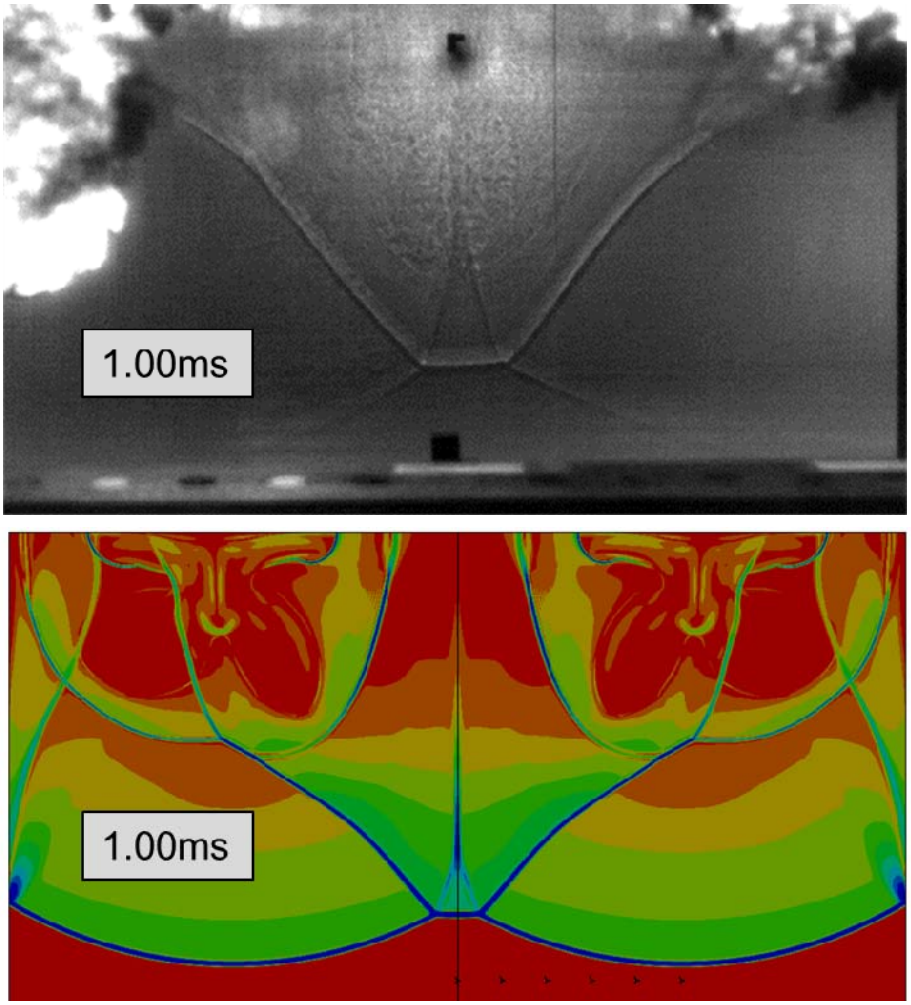

Figure 14 Comparison of high speed video shadowgraph (top) with corresponding digital Schlieren (bottom) from LS-DYNA density fringes.

4.6 Event 5 – Three 60 gram PE-4 Charges

The initial configuration for Event 5 with three 60 gram PE-4 charges suspended 1000 mm above the center and two outer pressure transducers, i.e. P06 and P1 & P11, is shown in Figure 15.

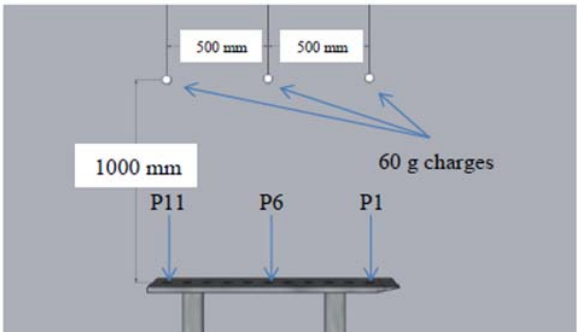

Figure 15 Configuration for Event 5 with three 60 gram PE-4 charges.(Figure 15 in Stojko et al.)

The result comparisons for Event 5 are shown in Figure 16. Only 2D axisymmetric results are possible for this multiple charge configuration. The maximum pressures are 1344 and 1336 kPa for P06 and the 2D model, respectively, and the TOA are similar with 1.025 and 0.997 milliseconds. For this event the central gauge and the simulation are nearly identical.

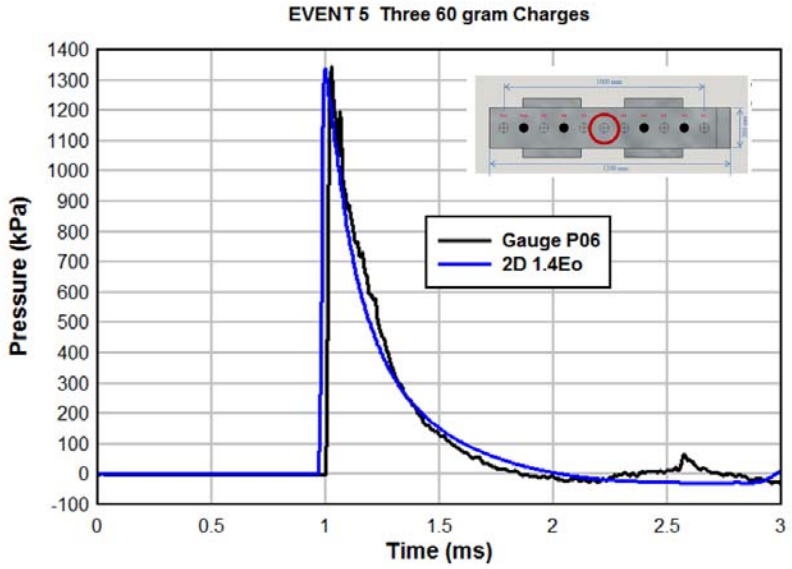

Figure 16 Comparison of pressure histories for Event 5 three 60 gram charge of PE-4 at the center gauge P06.

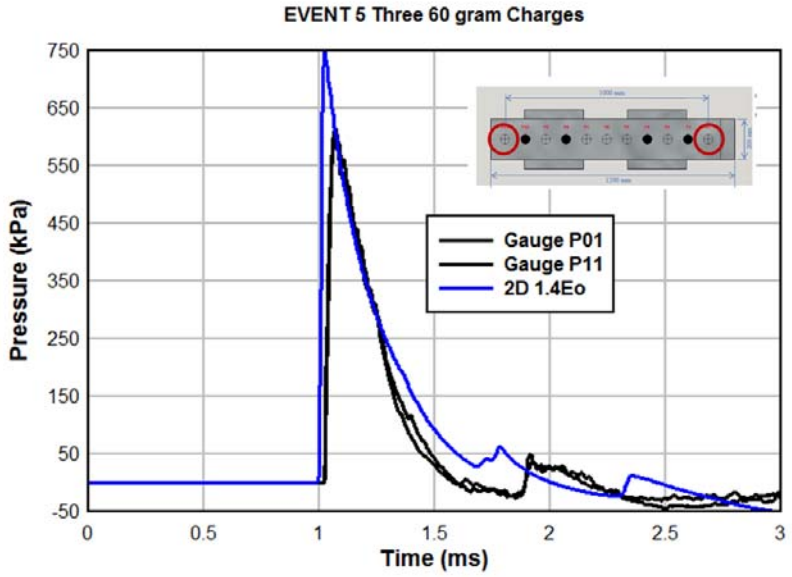

Figure 17 Comparison of pressure histories for Event 5 three 60 gram charge of PE-4 at the end gauges P01 and P11.

There was no repeat test for Event 5, but the two end gauges P01 and P11 serve as duplicate measurements due to symmetry. Figure 17 shows the two end gauge pressure histories and the 2D axisymmetric simulation result. The average maximum measured pressure is 611 kPa and the simulation maximum pressure s 751 kPa or 23% larger. The TOAs differ slightly with 1.07ms for the measurements and 1.02 for the simulation.

As with Event 4, in Event 5 the central gauge pressure history is well predicted by the simulation, but the outer gauges are significantly under predicted. This discrepancy remains a mystery.

Solution using Mapping **–** An alternative method for solving blast problems requiring large air domains is to use the LS-DYNA mapping feature: *INITIAL_ALE_MAPPING. This allows the user to solve for the initial detonation using a dense mesh within a limited air domain in the vicinity of the explosive and subsequently map that blast solution onto a more coarse mesh to continue the simulation. This is the approach that will be used for Event 6 where a 3D mesh is required as there is no axis of symmetry for the three charges on a circular arc.

To demonstrate the implementation of this feature, Event 5 was simulated again using a mapping of the 1D spherical 60 gram charges onto the 2D axisymmetric mesh. Figure 18 shows the initial 2D model configuration at 0.15ms, i.e. before the two explosive charge domains interact.

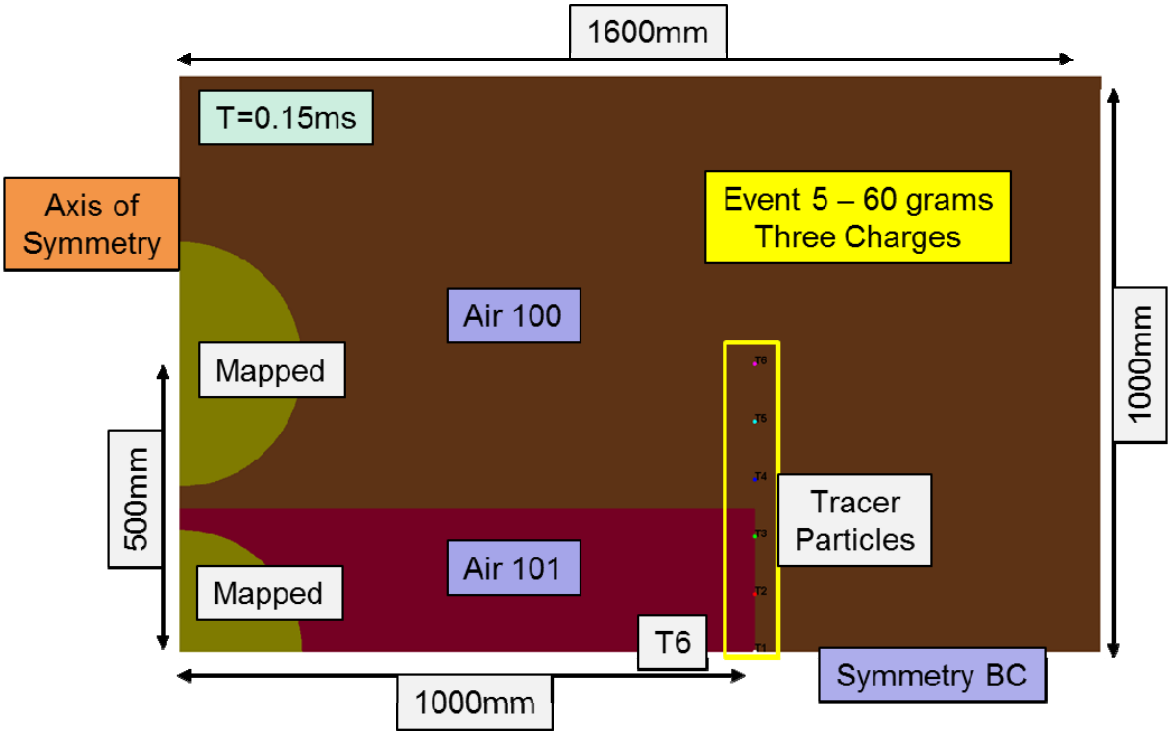

Figure 18 Illustration of 2D axisymmetric model using mapped 1D spherical solutions.

When multiple mappings are required, as in Event 5 with three 60 gram charges, care must be taken that the serial application of the mapping does not overwrite all or a portion of the previous mapping. Two approaches for generating the 1D spherical solutions are available:

1. Create a 1D mesh that does not extend beyond half the charge separation distance, i.e. 250 mm, and map that solution onto the 2D air domain twice.
2. Use a 1D mesh that extends beyond the half charge separation distance, but map that solution onto two different air domains, e.g. Air PID=100 and Air PID=101.

Since the 1D spherical solution for the 1000 mm mesh with a 60 gram charge already existed, use was made of the second mapping option. In this case, the 1D spherical solution was run for 0.15ms, i.e. the time at which the blast wave approached a radius of 250 mm.

Then two mapping keywords were included in the 2D simulation input:

```
$
*INITIAL_ALE_MAPPING
$  PID TYP AMMSID
   101, 1, 10101
$   XO   YO   ZO VECID ANGLE
```

```
   0.0, 0.0, 0.0, 222
$
*INITIAL_ALE_MAPPING
$  PID TYP AMMSID
   100, 1, 10100
$   XO   YO     ZO VECID ANGLE
   0.0, 500.0, 0.0, 222
$
```

where the AMMSID=10101 consists of the explosive PID=10 and Air PID=101 and similarly AMMSID=10100 consists of the explosive PID=10 and Air PID=100.

Figure 19 show the essentialy identical simulation results for the pressure at the central gauge location P06 with and without mapping.

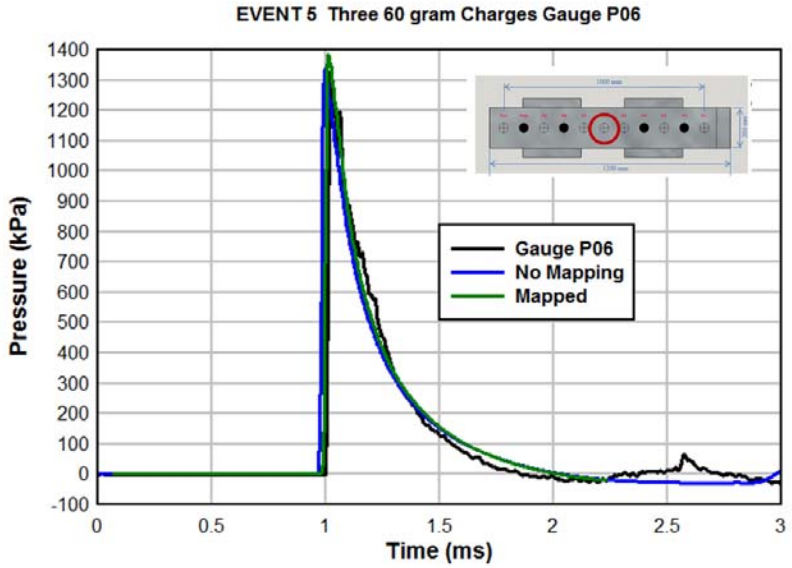

Figure 19 Comparison of 2D axisymmetric model pressure at central gauge P06 without and with mapping.

4.7 Event 6 – Three 60 gram PE-4 Charges on a Circular Arc

The initial configuration for Event 6 with three 60 gram PE-4 charges arranged on a 1000 mm radius above the target plate is shown in Figure 20.

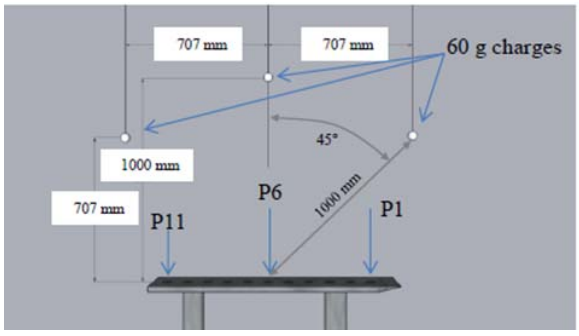

Figure 20 Configuration for Event 6 with three 60 gram PE-4 charges on a circular arc.

Although there are two planes of symmetry for Event 6, i.e. through the center charge and the gauge P6 and center of all three charges and the target plate, there is no axis of symmetry, so a 3D mesh is necessary.

Figure 21 shows the configuration of the 3D model used for the mapped simulation of Event 6. The symmetry planes are YZ plane passing through the center of the middle charge and XY plane passing through the center of the mapped charges. The mesh uses a ratio generating technique to focus the small elements in the central core of the model. The smallest cubic element is 5 mm on a side with increasing element sizes in the X-direction beyond the tracer particle array and in the Y direction below the tracer particle array. Finally, larger elements are used in the YZ plane in the negative Z-direction. The total number of elements in the one eighth symmetric ratio model is 6.528×10^{6}. Not shown here is a mesh convergence study where the results from the minimum 5 mm cube ratio mesh were compared to those from a 10 mm cube ratio mesh. The comparison indicated the results were not converged at the 10 mm size. An effort to generate another ratio mesh using a 2.5 mm cube minimum size has challenged the mesh generating software.

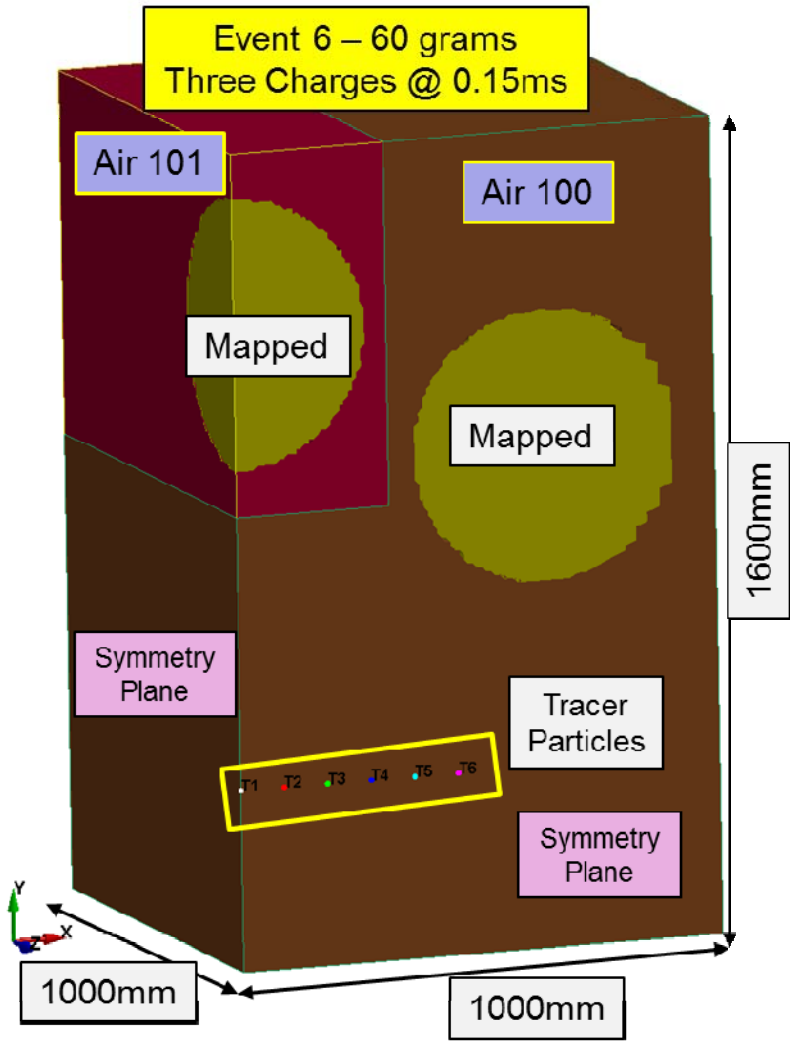

Figure 21 Illustration of 3D model for Event 6 with two planes of symmetry and two mapped 1D solutions.

The result comparisons for Event 6 are shown in Figure 22. Event 6 was repeated with maximum pressures are 1773 and 1644 kPa for P06 and 1784 kPa from the 3D model. The TOAs are similar with 0.993 and 0.977 milliseconds for the repeat measurements and 0.990ms for the 3D simulation.

Thus the model over predicts the average maximum pressure by 4% and is with 0.5% of the average measured TOA. Both of the percent differences are less than the coefficient of variation of the repeated measurements.

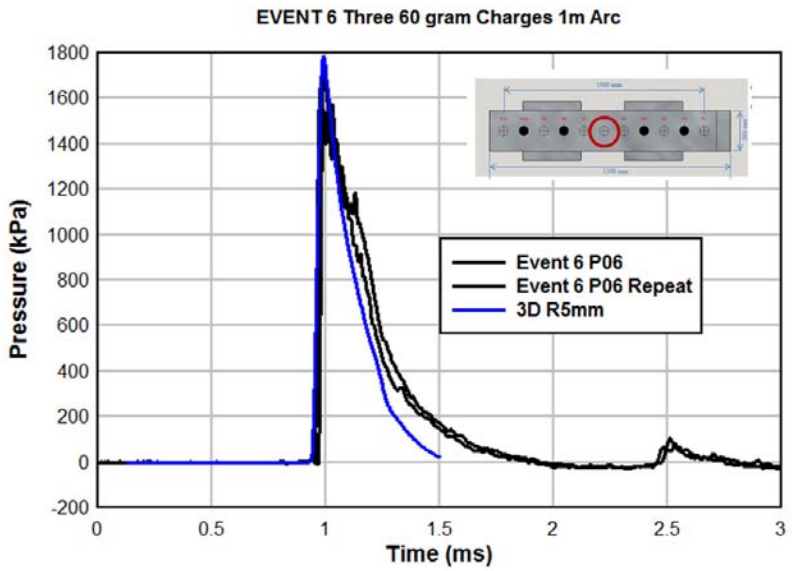

Figure 22 Comparison of repeated pressure histories at the center gauge P06 for Event 6 three 60 gram charge of PE-4 on a circular arc.

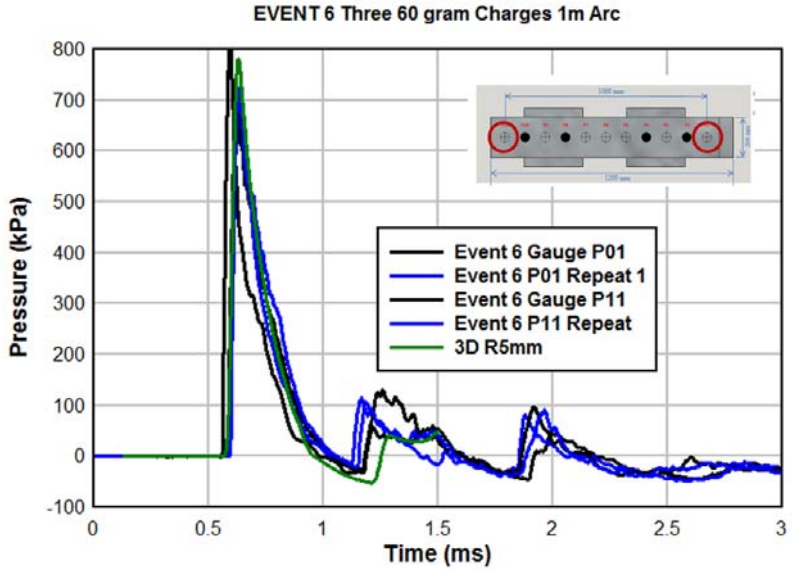

Figure 23 Comparison of repeated pressure histories at the end gauges P01 and P11 for Event 6 three 60 gram charge of PE-4 on a circular arc.

There was a repeat test for Event 6, so the two end gauges P01 and P11 also provide duplicate measurements due to symmetry, i.e. four independent measurements of the pressure history. Figure 23 shows the two end gauge repeated pressure histories and the 3D simulation result. The average maximum measured pressure is 739 kPa and the simulation maximum pressure is 781 kPa or 6% larger; The TOAs differ slightly with 0.62ms for the measurements and 0.63 for the simulation. Again, the maximum pressure difference between the average measurement and the simulation of 4% is less than the coefficient of variation of the data.

Unlike in the other two multiple charge simulations, i.e. Event 4 and Event 5, where the central gauge pressure history is well predicted by the simulation, but the outer gauges are significantly under predicted, in Event 6 both the central and outer gauges are well predicted by the simulation. One key difference between Events 4 & 5 and Event 6 is Events 4 & 5 lacked repeat tests. Likely a little more thought would produce other physical differences among these events.

5 Summary

The purpose of this study was to assess the suitability of the single and multiple charge experimental data as a validation database for numerical simulations. For the most part the data has been shown to agree quite well with the numerical simulation results presented in this manuscript.

To obtain initial agreement between the data and the simulations of the single 60 gram charge, a calibration study was performed via increasing the initial internal energy of the C-4 explosive used to represent the PE-4 explosive in the experiment. Once an energy calibration factor was established, it was used consistently for the larger mass single charges and the multiple 60 gram charge experiments. While the calibration factor fell short for the larger mass single charges, it worked well for the multiple 60 gram charge simulations.

A discrepancy was noted for two of the three multiple charge experiments between comparisons at the center pressure gauges and the symmetric outer gauges, i.e. the center gauge pressure was predicted well by the simulation, but for the outer gauges the comparison was less favorable. However for multiple charge Event 6 – three 60 gram charges on a circular arc – both the center and outer gauge comparison difference were within the coefficient of variation of the data.

6 References

Stojko, S., J. Freundt, J.G. Anderson and T. Delaney (2018) “Experimental Characterisation of the Interaction of Shock Waves from Multiple High Explosive Charges,” Presented at the 25th Military Aspects of Blast and Shock (MABS), The Hague, Netherlands, September 2018.

Bogosian, D., M. Yokota and S. Rigby (2016) “TNT Equivalence of C-4 and PE4: A Review of Traditional Sources and Recent Data,” Presented at the 24th Military Aspects of Blast and Shock (MABS), Halifax, Nova Scotia, Canada, September 2016

7 Appendix – Mesh Convergence

The simplest model for Events 1-3 is 1D spherical model using beam elements along a length 1000 mm with the distant radius constrained from radial motion. A tracer particle is located in the element nearest the constrained node representing pressure gauge P6. As noted previously, this configuration cannot account for late time pressure decay as the finite width pressure gauge array provides for pressure relief from the two nearest edges only 100 mm away from the pressure transducer.

Figure 24 shows a mesh refinement result for the 1D spherical model using 0.5 and 1 mm uniform mesh sizes. The two pressure histories are essentially identical with maximum pressures of 347.7 and 341.3 kPa (1.8% difference). Based on this mesh refinement result, uniform 1 mm mesh will also be used in simulating Events 2 and 3. Note: the negative phase at about 3ms is terminated by the arrival of the secondary shock from the recompression and expansion of the detonation products.

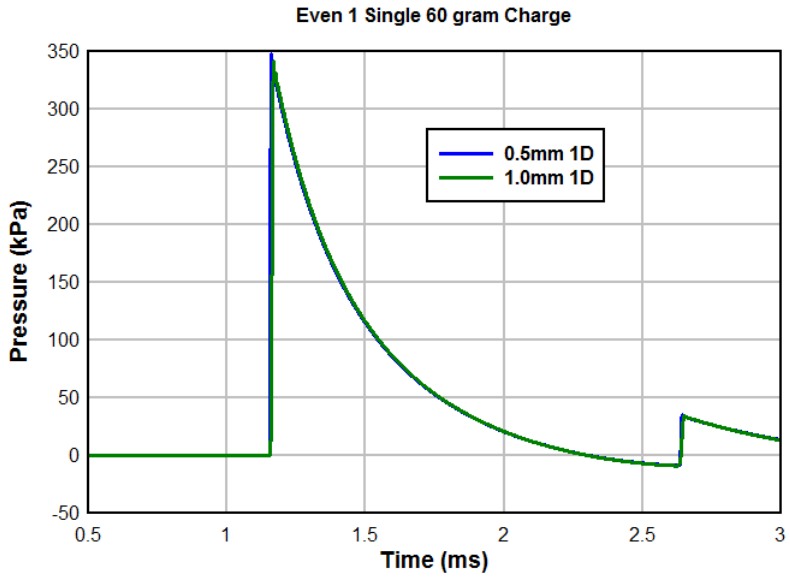

Figure 24 Mesh refinement for 1D spherical simulation of Event 1.

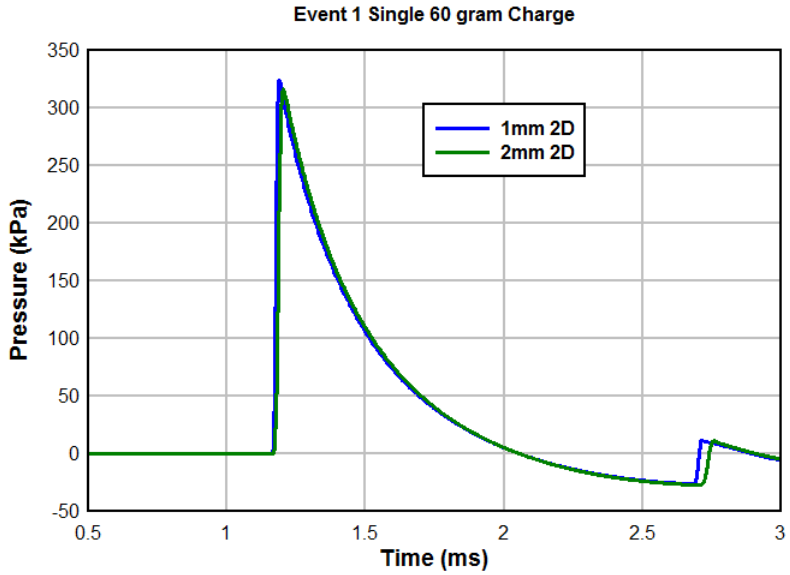

Figure 25 Mesh refinement for 2D axisymmetric mesh of Event 1.

Figure 25 shows a mesh refinement result for the 2D axisymmetric model using 1 and 2 mm uniform mesh sizes. The two 2D pressure histories are essentially identical with maximum pressures of 324.4 and 316.6 kPa (2.4% difference). Based on this mesh refinement result, uniform 2 mm meshes will also be used in 2D axisymmetric simulations of single charge Events 2 and 3 and multiple charge Events 4 and 5.

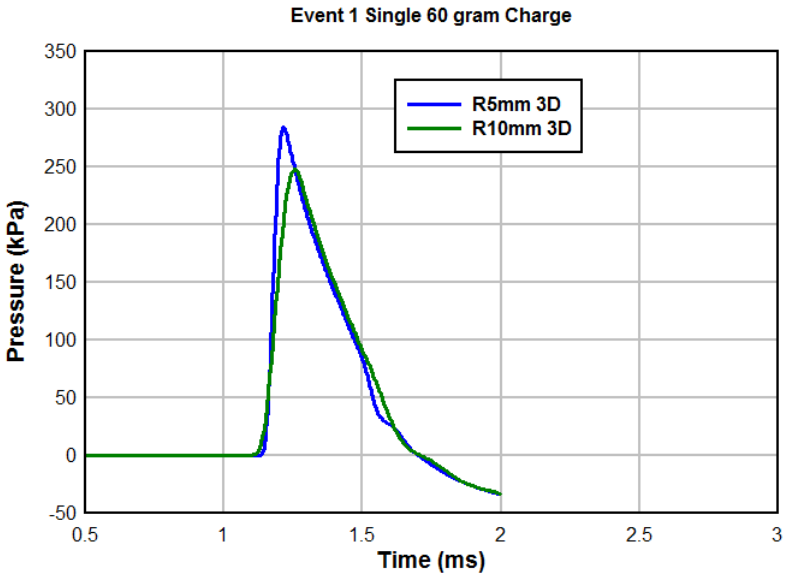

Figure 26 Mesh refinement for 3D mesh of Event 1.

Figure 26 shows a mesh refinement result for the 3D model using a ratio mesh with base elements sizes of 5 and 10 mm. The two 3D pressure histories differ significantly with maximum pressures of 284.2 and 247.5 kPa (12.9% difference). Clearly further mesh refinement is indicated as these two mesh results are not converged. However, based on limited CPU and memory resources an additional mesh refinement to a base mesh size of 2.5 mm is not currently possible. Thus the ratio mesh using the 5 mm base element will be used in 3D simulations of single charge Event 1 and multiple charge Event 6.

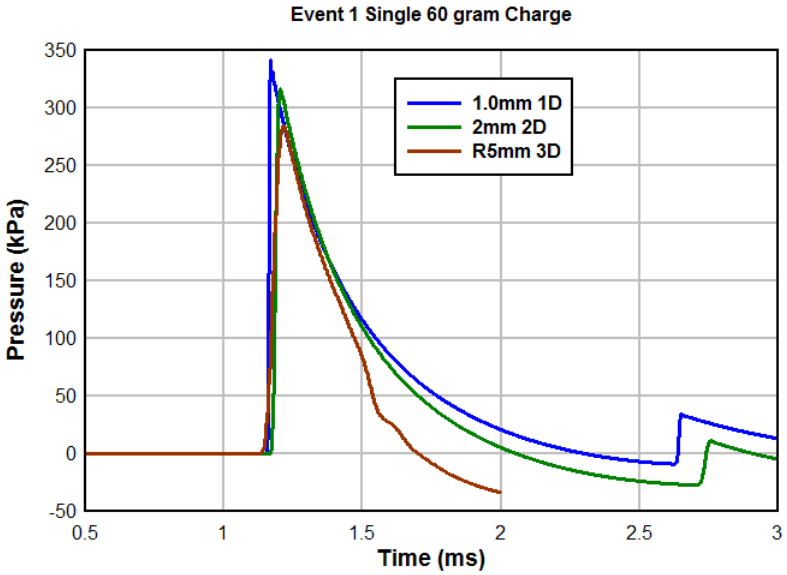

Figure 27 Comparison of 1D-2D-3D models of Event 1.

Figure 27 compares the results for the three geometric models of Event 1, i.e. 1D, 2D and 3D. As already indicated, there is decreasing accuracy in representing the maximum pressure as the number of special dimensions and corresponding mesh sizes are increased. However, the TOA's remain relatively constant. Finally, note the 3D simulation has significantly different pressure decay and transitions into the negative pressure phase much sooner than either the 1D or 2D simulations. This is the effect of relief waves from the sides of the target plate that are only 100 mm away from the tracer

particle at the center of the pressure transducer array. The 3D model is the only geometry that accounts for the relief wave effects.

8 Appendix – Alternative JWL EOS Parameters

Jing Ping Lu of DST offered two alternative sets of JWL equation of state parameters for representing PE-4. These were used in the 1D spherical LS-DYNA model of Event 1 with a 1mm uniform mesh. The results are shown in Figure 28 also with the result from ConWep, which uses a TNT equivalent mass of 1.28, the original LLNL Handbook parameters and the calibrated version with the initial internal energy increased by 40%. The JWL EOS parameters are list in Table 1.

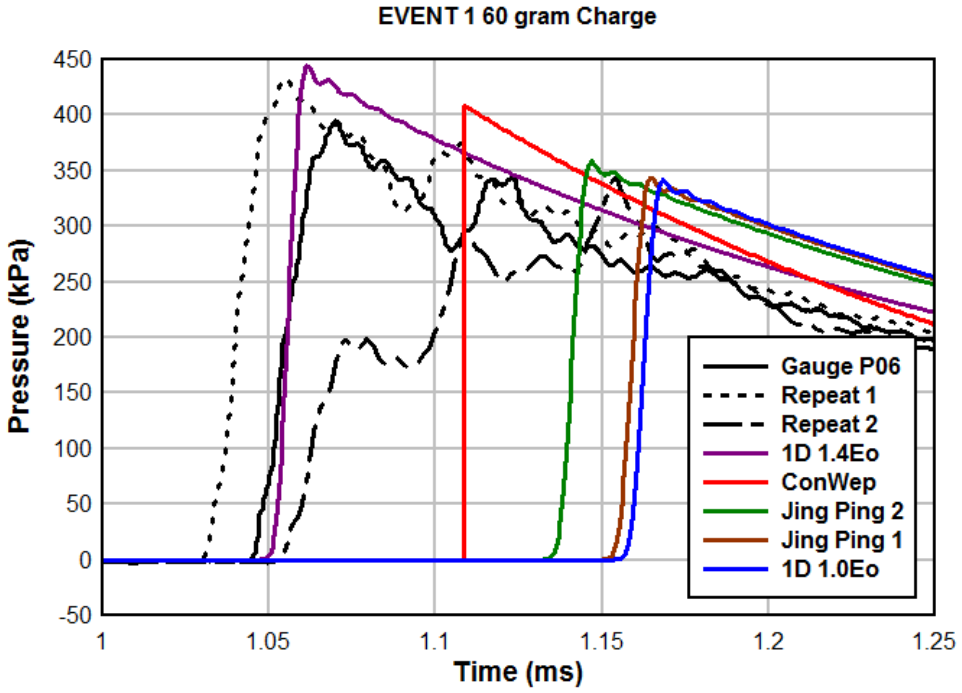

Figure 28 Comparison of three repeat Event 1 experiments pressure histories from ConWep and four alternate sets of JWL EOS parameters.

Table 1 Alternate JWL EOS parameters for PE-4.

	A (GPa)	B (GPa)	R1	R2	OMEG	Eo (GPa)	Vo
Jing Ping 1	597.4	13.90	4.5	1.5	0.320	8.70	1
Jing Ping 2	774.0	6.67	4.83	1.07	0.284	9.38	1
LLNL	609.8	12.95	4.5	1.4	0.25	9.00	1
1.4Eo	609.8	12.95	4.5	1.4	0.25	12.60	1

9 Appendix – Material Models and Equations of State

9.1 Air

```
*MAT_NULL
$    MID     RO        PC     MU     TEROD   CEROD   YM   PR
     100, 1.29e-6,  0.0,  0.0,  0.0,    0.0
$
$========1=========2=========3=========4=========5=========6========
=7
$                                  EOS CARDS
```

```
$========1=========2=========3=========4=========5=========6========
=7$
$  Properties for Air
$
*EOS_Linear_Polynomial
$ EOSID  C0    C1   C2   C3   C4   C5  C6
   100 ,  0.0, 0.0, 0.0, 0.0, 0.4, 0.4, 0.0
$  e0    v0
  0.25, 1.0
$
```

9.2 C-4 from LLNL Explosive Handbook

```
*MAT_HIGH_EXPLOSIVE_BURN
$ MID    RO          D         PCJ    BETA
 1080, 1.601-3,  8.193e3,   2.8E4,  0.0
$
$========1=========2=========3=========4=========5=========6========
=7
$                                EOS CARDS
$========1=========2=========3=========4=========5=========6========
=7
$
$
*EOS_JWL
$ EOSID     A         B       R1    R2    OMEG    E0     V0
 1080 , 6.098E5, 1.295E4,  4.5,  1.4,   0.25,  9.0E3, 1.0
$
```